Communication: Quantum molecular dynamics simulation of liquid para-hydrogen by nuclear and electron wave packet approach.

AUTHOR(S):

Hyeon-Deuk, Kim; Ando, Koji

Communication: Quantum molecular dynamics simulation of liquid para-hydrogen by nuclear and electron wave packet approach

Kim Hyeon-Deuk and Koji Ando

Citation: The Journal of Chemical Physics **140**, 171101 (2014); doi: 10.1063/1.4874635
View online: http://dx.doi.org/10.1063/1.4874635
View Table of Contents: http://scitation.aip.org/content/aip/journal/jcp/140/17?ver=pdfcov
Published by the AIP Publishing

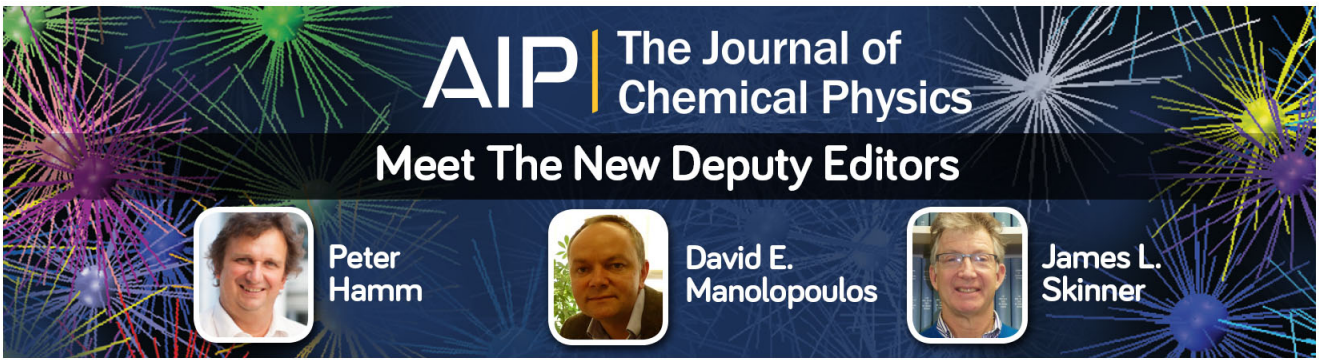

THE JOURNAL OF CHEMICAL PHYSICS **140**, 171101 (2014)

Communication: Quantum molecular dynamics simulation of liquid para-hydrogen by nuclear and electron wave packet approach

Kim Hyeon-Deuk[1,2,a)] and Koji Ando[1]
[1]*Department of Chemistry, Kyoto University, Kyoto 606-8502, Japan*
[2]*Japan Science and Technology Agency, PRESTO, 4-1-8 Honcho, Kawaguchi, Saitama 332-0012, Japan*

(Received 1 April 2014; accepted 22 April 2014; published online 2 May 2014)

Liquid para-hydrogen (p-H_2) is a typical quantum liquid which exhibits strong nuclear quantum effects (NQEs) and thus anomalous static and dynamic properties. We propose a real-time simulation method of wave packet (WP) molecular dynamics (MD) based on non-empirical intra- and inter-molecular interactions of non-spherical hydrogen molecules, and apply it to condensed-phase p-H_2. The NQEs, such as WP delocalization and zero-point energy, are taken into account without perturbative expansion of prepared model potential functions but with explicit interactions between nuclear and electron WPs. The developed MD simulation for 100 ps with 1200 hydrogen molecules is realized at feasible computational cost, by which basic experimental properties of p-H_2 liquid such as radial distribution functions, self-diffusion coefficients, and shear viscosities are all well reproduced.
 [http://dx.doi.org/10.1063/1.4874635]

Liquid para-hydrogen (p-H_2) is a typical quantum liquid, which exhibits anomalous properties especially at low temperature. Due to the strong nuclear quantum effect (NQE), liquid p-H_2 shows broad radial distribution functions (RDFs) and rapid diffusion properties even at low temperature, which cannot be reproduced by the classical simulation approaches.[1–6] Hydrogen is of primary importance not only in the fundamental condensed phase physics but also in its potential applications as energy source without harmful by-products. It is therefore important to establish an *a priori* computational method to predict the anomalous properties of p-H_2 liquids.

Methods suitable for numerical simulations of real p-H_2 ensembles have been proposed using the path integral Monte Carlo (PIMC),[1,2] linearized semiclassical initial value representation (LSC-IVR),[7,8] centroid molecular dynamics (CMD),[3,4,6] ring-polymer molecular dynamics (RPMD),[9] and the thermal Gaussian molecular dynamics (TGMD).[10] These all are based on the imaginary-time path-integral theory, and the latter four have been implemented for calculations of time correlation functions (TCFs) accounting for particularly important NQEs such as zero-point energy (ZPE) effect. They unanimously adopted the Silvera-Goldman potential[11] which assumes that the p-H_2 molecules are a spherically symmetric particle in the rotational ground state. This spherical model combined with the above quantum simulation methods has well reproduced the static and dynamical properties of liquid p-H_2.[1–6,9,10] We thus consider that the next step is to treat the interaction potential in less empirical way.

We have recently developed an efficient theoretical framework of a non-Born-Oppenheimer (non-BO) nuclear and electron wave packet (NWP and EWP) method non-perturbatively taking into account the NQEs such as nuclear delocalization and ZPE, and applied it to the intra- and inter-molecular energies of a hydrogen dimer.[12] In this Communication, we extend it to a real-time condensed-phase simulation method of nuclear and electron wave packet molecular dynamics (NEWPMD) for liquid p-H_2.

The NEWPMD approach describes nuclei by floating and breathing Gaussian WPs via the time-dependent Hartree approach, and EWPs by the perfect-pairing (PP) valence bond (VB) theory that appropriately treats the Pauli exclusion energy. The combination of EWP and PP VB has been demonstrated to yield accurate potential energy curves for H_2, LiH, CH_2, and H_2O.[12–14] We start by considering a H_2 dimer and denote the four electrons (4e) by a, b, c, and d, and the four nuclei (4n) by A, B, C, and D. Here, the nuclei (A, B) and electrons (a, b) form one hydrogen molecule, while the remaining (C, D) and (c, d) compose another hydrogen molecule. The time-dependent total wave function $\psi(t)$, where the EWP pairs (a, b) and (c, d) are coupled in the singlet configuration, is introduced as

$$\psi(t) = \mathcal{A}[\phi_a(\mathbf{q}_1)\phi_b(\mathbf{q}_2)\phi_c(\mathbf{q}_3)\phi_d(\mathbf{q}_4)\Theta(1,2,3,4)] \times \Phi_A(\mathbf{Q}_1)\Phi_B(\mathbf{Q}_2)\Phi_C(\mathbf{Q}_3)\Phi_D(\mathbf{Q}_4), \quad (1)$$

where $\mathcal{A}$ is an antisymmetrizer for 4e.[13,14] For simplicity, $\hbar = 1$, an electron charge is unity and all the coordinates are mass scaled. The spin function $\Theta(1, 2, 3, 4)$ expresses the PP VB, $\Theta(1,2,3,4) = (\alpha(1)\beta(2) - \beta(1)\alpha(2))/\sqrt{2} \times (\alpha(3)\beta(4) - \beta(3)\alpha(4))/\sqrt{2}$. Each term in $\psi(t)$ is composed of the 3D symmetric (spherical) Gaussian WP basis functions. The nuclear wave function part is introduced by the Hartree product of NWPs;

$$\Phi_K(\mathbf{Q}_i) \equiv \left(\frac{1}{2\pi\Omega_K^2(t)}\right)^{\frac{3}{4}} \exp[X_K(\mathbf{Q}_i - \mathbf{R}_K(t))^2 + i\mathbf{P}_K(t)\cdot(\mathbf{Q}_i - \mathbf{R}_K(t))] \quad (2)$$

a)kim@kuchem.kyoto-u.ac.jp

with $X_K = (-1 + 2i\Pi_K(t)\Omega_K(t))/4\Omega_K^2(t)$ and the EWP in the electronic part of a form

$$\phi_k(\mathbf{q}_i) \equiv \left(\frac{1}{2\pi\rho_k^2}\right)^{\frac{3}{4}} \exp\left[-\frac{(\mathbf{q}_i - \mathbf{r}_k(t))^2}{4\rho_k^2}\right]. \quad (3)$$

The Gaussian NWP is specified by the WP center $\mathbf{R}_K(t)$, its width $\Omega_K(t)$, and their conjugate momenta $\mathbf{P}_K(t)$ and $\Pi_K(t)$, respectively. On the other hand, the Gaussian widths of EWPs, ρ_k, are assumed to be constant at 0.654 Å for electrons a and c and 0.370 Å for electrons b and d in the present MD simulation, i.e., the EWPs are frozen and do not breath. The values of EWP width are determined from a calculation on a H_2 dimer.[15] Further, the EWP centers $\mathbf{r}_k(t)$ depend on the hydrogen nuclear coordinates at each moment as $\mathbf{r}_a(t) = \mathbf{r}_b(t) = (\mathbf{R}_A(t) + \mathbf{R}_B(t))/2$ and $\mathbf{r}_c(t) = \mathbf{r}_d(t) = (\mathbf{R}_C(t) + \mathbf{R}_D(t))/2$. The EWPs are not evolved variationally, but instead can instantly adjust their widths and positions to NWP dynamics at each moment. It is assumed that EWP breathing itself is small enough to be neglected compared to the total EWP width, and that the timescale of EWP dynamics is naturally much shorter than the timescale of NWP dynamics. The latter assumption is related to the BO approximation. These approximations, which have been validated in Ref. 15, greatly simplify the derivations of equations of motion (EOM) for hydrogen molecules from the time-dependent variational principle to yield,[15]

$$\begin{aligned} \dot{\mathbf{R}}_K &= \frac{\partial H_{\rm ext}}{\partial \mathbf{P}_K}, \quad \dot{\mathbf{P}}_K = -\frac{\partial H_{\rm ext}}{\partial \mathbf{R}_K}, \\ \dot{\Omega}_K &= \frac{1}{3}\frac{\partial H_{\rm ext}}{\partial \Pi_K}, \quad \dot{\Pi}_K = -\frac{1}{3}\frac{\partial H_{\rm ext}}{\partial \Omega_K}, \end{aligned} \quad (4)$$

with the extended Hamiltonian function,

$$\begin{aligned} H_{\rm ext} \equiv & \sum_K^{\rm A,B,C,D}\left[\frac{\mathbf{P}_K^2}{2M_{\rm nuc}} + \frac{3\Pi_K^2}{2M_{\rm nuc}} + \frac{3\hbar^2}{8M_{\rm nuc}\Omega_K^2}\right] \\ & + \langle V(\mathbf{q}_1, \mathbf{q}_2, \mathbf{q}_3, \mathbf{q}_4; \mathbf{Q}_1, \mathbf{Q}_2, \mathbf{Q}_3, \mathbf{Q}_4)\rangle, \end{aligned} \quad (5)$$

where $M_{\rm nuc}$ is a relative mass of a proton to an electron. Note that $\hbar$ has been retrieved here and hereafter. $\{\mathbf{R}_K, \mathbf{P}_K\}$ and $\{\Omega_K, \Pi_K\}$ can be regarded as conjugate coordinate and momentum pairs. The system dynamics can be described with the potential concept in this extended Hamiltonian.[16,17] In order to solve the EOM (4), we explicitly and non-perturbatively derive the potential expectation in Eq. (5) by the total wave function $\psi(t)$.[15] It is thus distinguished from most of the previous NWP approaches in which a potential surface was given in advance by a separate modeling and, in many cases, expanded quadratically around the moving NWP centers to perturbatively take into account the NQEs.[10,16,18–25]

Finally, we extend the above formulation for the 4e-4n system to a system composed of many-body hydrogen molecules. The extended Hamiltonian appearing in the EOM (4) for the $N_{\rm mol}$-body system is derived as[15]

$$\begin{aligned} H_{\rm ext}(N_{\rm mol}) \equiv & \sum_K^{N_{\rm nuc}}\left[\frac{\mathbf{P}_K^2}{2M_{\rm nuc}} + \frac{3\Pi_K^2}{2M_{\rm nuc}} + \frac{3\hbar^2}{8M_{\rm nuc}\Omega_K^2}\right] \\ & + \sum_{I>J}^{N_{\rm nuc}} \frac{1}{|\mathbf{R}_I - \mathbf{R}_J|}{\rm erf}\left(\frac{|\mathbf{R}_I - \mathbf{R}_J|}{2^{\frac{1}{2}}\left(\Omega_I^2 + \Omega_J^2\right)^{\frac{1}{2}}}\right) \\ & + \sum_{ab>cd}^{N_{\rm mol}} V^{ab,cd} - \sum_{ab}^{N_{\rm mol}}(N_{\rm mol} - 2)v^{ab}, \end{aligned} \quad (6)$$

where $N_{\rm nuc}$ and $N_{\rm mol}(=N_{\rm nuc}/2)$ are total numbers of nuclei and molecules, respectively. $V^{ab,cd}$ and v^{ab} are explicitly derived in Ref. 15. Two electrons a and b (or c and d) constituting one hydrogen molecule should be calculated as a pair in $V^{ab,cd}$, leading to the maximum number of summation $N_{\rm mol}$. Since the summation of $V^{ab,cd}$ by all molecular pairs causes multiple counting of the intramolecular electron energies, we need to subtract an energy of a single hydrogen molecule v^{ab}. Real-time microscopic trajectories of condensed-phase hydrogen molecules can be simulated using the EOM (4) with $H_{\rm ext}(N_{\rm mol})$ where no empirical parameter to specify the intra- and inter-molecular interactions was introduced.

To confirm whether the present simulation method describes a liquid state of p-H_2 correctly, we check the basic properties of the simulated p-H_2 system discussing the NQEs introduced by the NWPs. The liquid p-H_2 systems are composed of 1200, 576, and 252 molecules in a cubic simulation box with a periodic boundary condition. The liquid p-H_2 is set at the saturated vapor pressure; the molar volume is 27.0 $\times 10^{-6}$ m^3/mol and 32.0 $\times 10^{-6}$ m^3/mol at 14 K and 25 K, respectively.[3] In the cooling and equilibration runs, we make only the atomic center momentum degrees of freedom, $\mathbf{P}_K(t)$, influenced by the heat bath set by the velocity scaling thermostat and Berendsen methods with $T = 14$ K and 25 K. Other degrees of freedom are *freely* time-evolved by the EOM (4). After the careful cooling and equilibration runs, the whole phase space reaches the thermal equilibrium owing to heat conduction between the degrees of freedom controlled by the heat bath and the other degrees of freedom free from the heat bath. After the equilibration runs, we carry out the NVE (microcanonical) simulations for 100 ps. The computational costs for the current NEWPMD are reasonable since the EOM (4) representing the quantum hydrogens include only the auxiliary WP coordinates and momenta. The truncations of the electron exchange integrals in the interaction energy also contribute to reduce the computational cost.[15]

The average detailed structures of hydrogen molecules in the condensed p-H_2 liquid are calculated owing to the diatomic hydrogen structure described in our method. In Table I, the average microscopic structures of diatomic hydrogen molecules are listed and compared for different system size and temperatures. The average H–H bond length, $\langle r_{\rm HH}\rangle$, becomes longer in the liquid case than in the isolated free molecule case, which is nontrivial but agrees with the experimental finding in the low-pressure solid.[26] The calculated $\langle r_{\rm HH}\rangle$ of 0.762 Å is reasonably compared to the experimental result, 0.755 Å. Since the most stable solvation structure is

TABLE I. Average microscopic structures of hydrogen molecules. The numerical errors are smaller than the last significant figure. Stronger condensed-phase effects elongate H–H bond length r_{HH}. NWP width Ω has the clear correlation with r_{HH}. A molecular angle formed by two hydrogen molecules θ of 90° supports the most stable T-shape solvation configuration.

N_{mol}	T (K)	$\langle r_{HH}\rangle$ (Å)	$\langle\Omega\rangle$ (Å)	$\langle\theta\rangle$ (deg.)
1200	14	0.7619	0.065920	90.0
1200	25	0.7616	0.065916	90.0
576	14	0.7619	0.065920	90.0
576	25	0.7616	0.065916	90.0
252	14	0.7619	0.065920	90.0
252	25	0.7616	0.065916	90.0
1	0	0.7450	0.064861	...

the T-shape configuration drawn in Fig. S1 of the supplementary material,[15] the H–H bond of the right molecule is more elongated by the attraction from the electron distribution in the bonding region of the left H_2 molecule as the liquid structure becomes more condensed. Actually, the H–H bond is more stretched at 14 K than at 25 K; the lower temperature makes the p-H_2 liquid more structured as will be indicated in Fig. 1, which induces the longer H–H bond at 14 K. The averaged NWP width, $\langle\Omega\rangle$, is correlated to the H–H bond length $\langle r_{HH}\rangle$. As the H–H bond stretches, the NWP width becomes delocalized, and *vice versa*. This behavior, which has been observed and discussed in the hydrogen monomer and dimer cases,[12] thus remains in the liquid phase. The NWP width in the present model is primarily determined by the intramolecular bonding potential. In comparison, the thermal de Broglie wavelength of free translational motions of H_2 molecule is much larger, approximately 2.8 Å at 20 K. The accuracy of

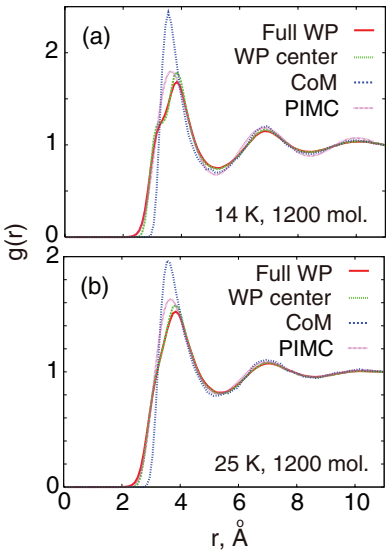

FIG. 1. RDFs with quantum delocalization of each NWP (red line), counted by centers of each NWP (green line), and defined by centers of hydrogen molecule mass (blue line). The peak positions, height, and width successfully reproduce the liquid structure of p-H_2 measured by the neutron scattering experiment. The PIMC data with the Silvera-Goldman potential were taken from Ref. 27. The shoulder appearing in the first peak reflects the diatomic structure of a hydrogen molecule in the first solvation shell. The peaks and valleys of the RDF become broader and deviate to the larger distance at the higher temperature. The current liquidized structure is obtained owing to the quantization of hydrogen nuclei introduced by the NWPs.

RDFs and diffusion constants to be shown below indicates that the quantum decoherence is in effect for translational motions in the liquid phase. The angular coordinate θ denotes an angle formed by two hydrogen molecules. The average molecular angle $\langle\theta\rangle$ listed in Table I are all 90°, supporting the most stable T-shape solvation configuration. All the average microscopic structures listed in Table I almost converge at the smallest system of 252 molecules.

Figure 1 shows the RDFs obtained from the NEWPMD at various system size and temperatures. In Figs. 1(a) and 1(b), we compare the three cases: (I) The RDF calculated with the quantum delocalization of each NWP (red line), (II) the RDF counted by the center of each NWP (green line), and (III) the RDF defined by the center of hydrogen molecule mass (blue line). The whole shape of the RDF (I) including all the peak positions, height and width almost agree well with the previous PIMC,[1,2,27] LSC-IVR,[7] and CMD[3,4,6] calculations and the neutron scattering experiments.[5,6] The shoulder appearing in the left part of the first RDF peak reflects the diatomic structure of a hydrogen molecule in the first solvation shell; the most stable solvation structure is the configuration drawn in Fig. S1 of the supplementary material,[15] and the nearest hydrogen atoms around the center hydrogen contribute to the shoulder around 3.25 Å. Though slightly, this shoulder is emphasized and the peak becomes narrower and higher in the RDF (II) which neglects the NWP delocalization in the RDF counting. The RDF (III) is quite different from the RDFs (I) and (II); the former first peak becomes much higher and deviates toward the shorter distance, vanishing the shoulder of the first peak appearing in the RDFs (I) and (II). This discordance suggests that a spherical approximation of a hydrogen molecule is invalid for the current diatomic picture. Comparison of Figs. 1(a) and 1(b) indicates that the peaks and valleys of the RDF become broader and deviate toward the larger distance at the higher temperature, while the position of the first peak does not change, in agreement with the previous CMD results.[3,4,6] In addition, the shoulder of the first RDF peak is weakened at the higher temperature, reflecting the less structured p-H_2 liquid. The direct comparisons with the PIMC results are also given in Fig. 1. The deviation around the first peak is mainly attributed to the appearance of the shoulder in the NEWPMD; in fact, the deviation is larger at 14 K than at 25 K. It is well known that the RDF obtained from the classical MD exhibits a much sharper and thus an entirely different distribution, implying that the classical liquid is more likely to be solidified compared with the quantum liquid.[4] The current quantization of the hydrogen nuclei introduced by the NEWPMD makes the intermolecular distance larger and makes the radial distribution much broader. The effective intermolecular attraction is reduced by the additional excluded volume effect and repulsive force caused by the hydrogen NWPs just as the liquid water case reported before.[24,25]

Figure 2 shows the self-diffusion coefficients[24,25] as a function of $N_{mol}^{-1/3}$ calculated in this work as well as the RPMD and TGMD results.[9,10] In general, a major deviation from a bulk self-diffusion coefficient follows:

$$D(N) = D(\infty) - \frac{2.837 k_B T}{6\pi\eta l} N_{mol}^{-1/3}, \qquad (7)$$

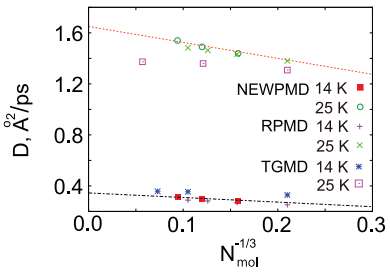

FIG. 2. Self-diffusion coefficients as a function of $N_{\mathrm{mol}}^{-1/3}$ compared with the RPMD and TGMD results. The self-diffusion coefficients are linearly proportional to $N_{\mathrm{mol}}^{-1/3}$ and increase quite rapidly with increasing the temperature. The fitting lines are $0.345 - 0.360N_{\mathrm{mol}}^{-1/3}$ (dashed-dotted line) and $1.65 - 1.25N_{\mathrm{mol}}^{-1/3}$ (dashed line). The estimated NEWPMD diffusion coefficients and shear viscosities sufficiently agree with the experimental data of liquid p-H_2 at the saturated vapor pressure. These agreements demonstrate that the current *temperature* definition, the kinetic temperature of the NWP center degrees of freedom, is physically valid.

for a cubic cell as was investigated analytically and numerically.[28,29] η is the shear viscosity, and $l = 3.55$ Å at 14 K and 3.76 Å at 25 K for the current molar volume.[9] As well as the RPMD and TGMD results, all the self-diffusion coefficients obtained from the NEWPMD depend linearly on $N_{\mathrm{mol}}^{-1/3}$ and thus can be fitted to Eq. (7). This behavior with the negative slope indicates that the "classical bubble" is not formed and thereby supports the adequacy of the present NEWPMD method to simulate the quantum liquid state; the self-diffusion coefficient of the classical hydrogen liquid decreases significantly with increasing the system box.[9,29] The self-diffusion coefficients of the infinite system obtained by extrapolating the NEWPMD data to $N_{\mathrm{mol}} \to \infty$ are $D(\infty) = 0.345$ Å^2/ps at 14 K and 1.65 Å^2/ps at 25 K, in agreement with the corresponding experimental values of 0.35 − 0.37 Å^2/ps at 14 K and 1.4 − 1.6 Å^2/ps at 25 K.[9,10] We can also estimate the shear viscosity η from the gradient of the linear fitting line. The resulting viscosities are $\eta = 2.28 \times 10^{-5}$ N s m^{-2} at 14 K and 1.10×10^{-5} N s m^{-2} at 25 K, again in agreement with the experimental shear viscosities of liquid p-H_2 at the saturated vapor pressure, 2.51 N s m^{-2} at 14 K and 0.943 N s m^{-2} at 25 K.[30] Figure 2 demonstrates that the NEWPMD self-diffusion coefficients increase quite rapidly with increasing the temperature. The self-diffusion coefficients become about five times larger by increasing the temperature only by less than twice. This can be explained by combined and correlated effects of the less structured liquid and the shorter H–H bond length in the higher temperature as discussed in Table I and Fig. 1.

The current results of temperature dependent self-diffusion coefficients are suggestive for adequate definition of thermodynamic *temperature* in the NEWPMD simulation which has not been fully understood.[24,25] While the quantum WP variables account for the NQEs, their extra dimensionality leads to an overcounting of quantum states if the phase space averaging is performed over both the WP center and width variables. Indeed, integration over all the NWP degrees of freedom to calculate average system energy in the Boltzmann distribution yields a surplus to the ZPE.[16] In the current NEWPMD simulations, the *temperature* is defined only by the kinetic temperature of WP center degrees of freedom assuming their canonical distribution even when embedded in a quantum WP simulation.[15] The assorted agreements of the self-diffusion coefficients and shear viscosities with the experiments demonstrate the validity of this definition since no microscopic adjusting parameter is introduced in the current NEWPMD.

In conclusion, we for the first time developed the combined NWP and EWP real-time MD simulation method without any empirical parameters for the hydrogen interaction energies, and applied it to the condensed-phase p-H_2 liquid. Each non-spherical hydrogen molecule in the NEWPMD has the intramolecular degrees of freedom of H_2. The computational costs for the current NEWPMD are quite reasonable. Nevertheless, the experimental basic properties of p-H_2 liquid such as the RDFs, self-diffusion coefficients, and shear viscosities were successfully reproduced, demonstrating that our NEWPMD can be an accurate and efficient quantum MD method to study condensed-phase p-H_2 systems.

K.H.D. thanks the financial supports from JST (PRESTO), and grant-in-aids for Scientific Research from Japan Society for the Promotion of Science (KAKENHI), Grant No. 24750016. K.A. acknowledges support from KAKENHI No. 22550012. We thank Professor A. Nakayama and Professor N. Makri for providing their PIMC RDF data.

[1] D. Scharf, G. J. Martyna, and M. L. Klein, Low Temp. Phys. **19**, 364 (1993) [Fiz. Nizk. Temp. **19**, 516 (1993)].
[2] M. Zoppi, M. Neumann, and M. Celli, Phys. Rev. B **65**, 092204 (2002).
[3] Y. Yonetani and K. Kinugawa, J. Chem. Phys. **120**, 10624 (2004).
[4] Y. Yonetani and K. Kinugawa, J. Chem. Phys. **119**, 9651 (2003).
[5] F. J. Bermejo, K. Kinugawa, C. Cabrillo, S. M. Bennington, B. Fak, M. T. Fernandez-Diaz, P. Verkerk, J. Dawidowski, and R. Fernandez-Perea, Phys. Rev. Lett. **84**, 5359 (2000).
[6] F. J. Bermejo, B. Fak, S. M. Bennington, K. Kinugawa, J. Dawidowski, M. T. Fernandez-Diaz, C. Cabrillo, and R. Fernandez-Perea, Phys. Rev. B **66**, 212202 (2002).
[7] J. A. Poulsen, G. Nyman, and P. J. Rossky, J. Phys. Chem. B **108**, 19799 (2004).
[8] J. Liu and W. H. Miller, J. Chem. Phys. **128**, 144511 (2008).
[9] T. F. Miller and D. E. Manolopoulos, J. Chem. Phys. **122**, 184503 (2005).
[10] I. Georgescu, J. Deckman, L. J. Fredrickson, and V. A. Mandelshtam, J. Chem. Phys. **134**, 174109 (2011).
[11] I. F. Silvera and V. V. Goldman, J. Chem. Phys. **69**, 4209 (1978).
[12] K. Hyeon-Deuk and K. Ando, Chem. Phys. Lett. **532**, 124 (2012).
[13] K. Ando, Bull. Chem. Soc. Jpn. **82**, 975 (2009).
[14] K. Ando, Chem. Phys. Lett. **523**, 134 (2012).
[15] See supplementary material at http://dx.doi.org/10.1063/1.4874635 for the complete theoretical derivations, simulation details, and additional figures of radial distribution functions and time-dependent diffusion coefficients.
[16] E. Heatwole and O. V. Prezhdo, J. Chem. Phys. **126**, 204108 (2007).
[17] Y. Shigeta, H. Miyachi, and K. Hirao, J. Chem. Phys. **125**, 244102 (2006).
[18] F. Grossmann, Chem. Phys. Lett. **262**, 470 (1996).
[19] F. Grossmann and T. Kramer, J. Phys. A **44**, 445309 (2011).
[20] S.-Y. Lee and E. J. Heller, J. Chem. Phys. **76**, 3035 (1982).
[21] M. H. Beck, A. Jackle, G. A. Worth, and H.-D. Meyer, Phys. Rep. **324**, 1 (2000).
[22] I. Burghardt, K. Giri, and G. A. Worth, J. Chem. Phys. **129**, 174104 (2008).
[23] D. V. Shalashilin and M. S. Child, J. Chem. Phys. **128**, 054102 (2008).
[24] K. Hyeon-Deuk and K. Ando, J. Chem. Phys. **131**, 064501 (2009).
[25] K. Hyeon-Deuk and K. Ando, J. Chem. Phys. **132**, 164507 (2010).
[26] P. Loubeyre, M. Jean-Louis, and I. F. Silvera, Phys. Rev. B **43**, 10191 (1991).
[27] A. Nakayama and N. Makri, J. Chem. Phys. **119**, 8592 (2003).
[28] B. Dunweg and K. Kremer, J. Chem. Phys. **99**, 6983 (1993).
[29] I.-C. Yeh and G. Hummer, J. Phys. Chem. B **108**, 15873 (2004).
[30] D. E. Diller, J. Chem. Phys. **42**, 2089 (1965).